

Multiple “time step” Monte Carlo simulations: Application to charged systems with Ewald summation

Katarzyna Bernacki^{a)}

Department of Chemistry and Center for Biomolecular Simulation, Columbia University, New York, New York 10027

Balázs Hetényi^{b)}

Department of Chemistry, Princeton University, Princeton, New Jersey 08544

B. J. Berne^{c)}

Department of Chemistry and Center for Biomolecular Simulation, Columbia University, New York, New York 10027

(Received 16 October 2003; accepted 1 April 2004)

Recently, we have proposed an efficient scheme for Monte Carlo simulations, the multiple “time step” Monte Carlo (MTS-MC) [J. Chem. Phys. **117**, 8203 (2002)] based on the separation of the potential interactions into two additive parts. In this paper, the structural and thermodynamic properties of the simple point charge water model combined with the Ewald sum are compared for the MTS-MC real-/reciprocal-space split of the Ewald summation and the common Metropolis Monte Carlo method. We report a number of observables as a function of CPU time calculated using MC and MTS-MC. The correlation functions indicate that speedups on the order of 4.5–7.5 can be obtained for systems of 108–500 waters for $n = 10$ splitting parameter. © 2004 American Institute of Physics. [DOI: 10.1063/1.1755195]

I. INTRODUCTION

Computer simulations of charged systems dominated by long range electrostatic interactions are becoming more important in the study of biological systems. The long-range electrostatic interactions in molecular systems make simulations computationally intensive. The dynamics in those systems usually have a multiple time scales nature.¹ Since the evaluation of the long-range potential is the most CPU intensive part of a simulation, minimizing the computational cost of that part can lead to a significant reduction in simulation time.

In a recent paper,² we have introduced a novel rapidly convergent Monte Carlo technique, the multiple “time step” Monte Carlo (MTS-MC). MTS-MC is similar in principle to multiple time-scale molecular dynamics;^{3–6} both take advantage of the separation of the potential into short and long range components. We have performed² a comparison of the standard Metropolis Monte Carlo (MMC) to MTS-MC. The diffusion in the configuration space as a function of CPU time was used as an efficiency criterion for the two methods that were evaluated. Our calculations showed savings in CPU time up to factors of 5.6 for our largest system of 1000 particles. We have also studied the scaling of CPU time as a function of system size, and have shown that for system sizes up to 1000 particles, the linear term dominates.

Long-range electrostatic interactions can be incorporated into calculations by using the Ewald summation method.⁷ It seems natural to use Ewald summation as a basis for separating short and long-range potentials in a MTS-MC split; the real-space part of the Ewald sum can be considered to be short ranged and the reciprocal-space part is included in the long-range interactions.^{8–10} An alternative way to split up the Ewald sum is to assign the entire Coulomb interactions between the nearby pairs to the short-range potential, including both real- and reciprocal-space contributions.^{1,5} Then the interactions between distant particles can be assigned to the long-range potential. This way all the interactions are subdivided based on the distance between atoms, regardless of whether they belong to real- or reciprocal-space.

In this work, we compare the radial distribution functions, dipole–dipole and energy correlation functions, and the dielectric constants calculated by MTS-MC and MMC. The effect of system size on the scaling of the new scheme is examined with systems of 108, 256, and 500 water molecules. The results indicate that the MTS-MC scheme can be efficiently used to include long-range electrostatic interactions in simulations of condensed media.

We also show that in order to achieve the same speedup for larger water systems as for the original 108 molecules, the real- and reciprocal-space cutoffs (r_c and k_c) had to be, respectively, decreased and increased. Decreasing cut-off radius r_c and increasing the screening parameter κ puts more work into the reciprocal-space component making the new method even faster. The problem of scaling Ewald parameters could be eliminated by using techniques like particle mesh Ewald (PME)^{11,12} and particle–particle–particle Mesh Ewald (P3ME)^{1,13–16} that are capable of performing the

^{a)}Present address: Department of Pharmaceutical Chemistry, UCSF, San Francisco, CA 94143.

^{b)}Present address: SISSA, International School for Advanced Study, via Beirut 2-4, 34014, Trieste, Italy.

^{c)}Electronic mail: berne@chem.columbia.edu

reciprocal-space sum more efficiently than the real-space sum. Thus, for large scale biomolecular applications, these techniques would be complementary to both Monte Carlo methods.

In Sec. II, we describe the multiple “time step” Monte Carlo (MTS-MC) method. In Sec. III, we present the splitting of Ewald sum in the framework of MTS-MC algorithm and scaling of Ewald parameters. In Sec. IV, we present the simulation details and show results for simple point charge (SPC) water simulations. Results are summarized in Sec. V.

II. MULTIPLE “TIME STEP” MONTE CARLO (MTS-MC)

A. Sampling procedure

Since we described the method in detail in a recent paper,² in this section we only present an outline of the MTS-MC scheme. The functionality of the MTS-MC method relies on the fact that the potential energy parts vary at different rates which enables us to evaluate the slowly varying contribution to the potential energy less frequently than the quickly varying ones. We suppose that the potential energy of the system can be written as the sum of two additive terms

$$V(\mathbf{x}) = V_S(\mathbf{x}) + V_L(\mathbf{x}), \quad (1)$$

where $V_S(\mathbf{x})$ is the rapidly varying part, the short-range potential energy, and $V_L(\mathbf{x})$ is the slowly varying part, the long-range potential energy. As in the multiple time step MD methodology, we wish to construct a sampling scheme in which $V_L(\mathbf{x})$ is evaluated less frequently than $V_S(\mathbf{x})$. We have proposed an algorithm that can be summarized by the following procedure:

- Step 1: For a given configuration \mathbf{x} , we evaluate $V_S(\mathbf{x})$ and $V_L(\mathbf{x})$. We duplicate the configuration \mathbf{x} , such that initially $\mathbf{x}_{\text{old}} = \mathbf{x}$ and $\mathbf{y}_{\text{old}} = \mathbf{x}$, then we use \mathbf{y}_{old} as the initial configuration in Step (2).
- Step 2: We generate a new configuration \mathbf{y}_{new} by performing a uniform random move (displacement and rotation) of a single molecule. We evaluate $V_S(\mathbf{y}_{\text{new}})$. Then, the new configuration \mathbf{y}_{new} is accepted or rejected according to the following acceptance probability

$$A_S(\mathbf{y}_{\text{new}}|\mathbf{y}_{\text{old}}) = \min[1, e^{-\beta[V_S(\mathbf{y}_{\text{new}}) - V_S(\mathbf{y}_{\text{old}})]}]. \quad (2)$$

The acceptance probability in Eq. (2) only depends on $V_S(\mathbf{x})$, the short-range potential energy. The procedure described in this step is defined as an “S-move.”

- Step 3: Repeat Step (2) n times where n is defined as the MTS-MC “splitting parameter.” After n S-moves, the final configuration is \mathbf{x}_{new} .
- Step 4: We evaluate $V_L(\mathbf{x}_{\text{new}})$. We accept or reject the resulting configuration by an acceptance probability constructed as

$$A_L(\mathbf{x}_{\text{new}}|\mathbf{x}_{\text{old}}) = \min[1, e^{-\beta[V_L(\mathbf{x}_{\text{new}}) - V_L(\mathbf{x}_{\text{old}})]}]. \quad (3)$$

The acceptance probability in Eq. (3) only depends on $V_L(\mathbf{x})$, the long-range potential energy. In the case of acceptance, the new configuration is \mathbf{x}_{new} . In the case of rejection, we go back to the configuration that we started with in Step (1), \mathbf{x}_{old} .

The above procedure is defined as an “L-move.” A pass will be generated by performing N L-moves where N is the number of molecules in the system. Estimators for observables should be evaluated for configurations that have been generated by L-moves. In the previous paper,² we have shown that the configurations generated by L-moves obey detailed balance. Thus, for evaluating observables, only the results of L-moves can be used.

The potential advantage of the scheme presented above is that it allows the calculation of statistically independent configurations in a manner such that $V_L(\mathbf{x})$ (the more expensive potential in our case) is evaluated fewer times than in the standard Monte Carlo scheme. The algorithm can be generalized to more than two stages if the potential is separable into more than two length scales.

III. EWALD METHOD

A. Combining MTS-MC method with the Ewald sum

In MD simulations, when devising a potential break-up, one major constraint is energy conservation; in the present method, the break-up is not constrained by energy conservation. A “bad break-up” from the MC standpoint affects only convergence or the “diffusion efficiency.” In this section, we discuss the implementation of our new MC algorithm for a system consisting of the simple point charge (SPC)¹⁷ water molecules using Ewald sum.^{7,18,19} Many different break-ups are possible using the Ewald sum. The break-up that we have implemented is simple and straightforward.

The energy for electrostatic interactions between charged particles in a periodic system can be written as⁷

$$V^{\text{el}} = \frac{1}{2} \sum_{\mathbf{n}} \sum_i \sum_j' \frac{q_i q_j}{|\mathbf{r}_{ij} + \mathbf{n}L|}, \quad (4)$$

where q_i and q_j are the charges. The sum over \mathbf{n} is the sum over all integer vector points, $\mathbf{n} = (n_x, n_y, n_z)$, and L is the edge length of the cubic unit cell. We omit $i=j$ for $\mathbf{n}=0$. This sum is conditionally convergent for long-range potentials, and it is expensive to compute. The final electrostatic energy is rearranged into two parts—part of it is summed in real space, and the rest is summed in Fourier space—as follows:

$$V^{\text{el}} = \frac{1}{2} \sum_i \sum_{j \neq i} A_{ij} + \frac{1}{2\pi L^3} \sum_i \sum_j \sum_{\mathbf{k} \neq 0} B_{ij} - \frac{\kappa}{\sqrt{\pi}} \sum_i q_i^2, \quad (5)$$

where

$$A_{ij} = q_i q_j \frac{\text{erfc}(\kappa r_{ij})}{r_{ij}}, \quad (6)$$

$$B_{ij} = \frac{4\pi^2}{k^2} q_i q_j e^{-k^2/4\kappa^2} \cos(\mathbf{k} \cdot \mathbf{r}_{ij}),$$

and $\text{erfc}(\mathbf{x})$ is a complementary error function which decays to zero with increasing \mathbf{x} . In Eqs. (5) and (6) metallic boundary conditions are used. The second term is a sum over reciprocal vectors $\mathbf{k} = 2\pi\mathbf{n}/L$. A large value of the screening

parameter κ represents a sharp distribution of charge, and in order to model it, many terms in the k -space summation must be included.⁷

The first term in Eq. (5) includes primarily short-range interactions, and the second term results from Fourier expansion of the potential due to an infinite array of Gaussian charges, and is considerably longer-range than the real-space sum.¹

Assuming that the long-range interactions may be updated less frequently than the short-range ones, it seems natural to separate the real- and k -space sums in the MTS-MC split. Here, for simplicity, the straightforward split between the real-space part of the Ewald sum (short-range) and the reciprocal part (long-range) is used. The real-space and k -space parts of the potential can be separated in the following way:

$$V_{ij}^{\text{el}} = V_{ij}^{\text{rs}} + V_{ij}^{\text{ks}} + V_{ij}^{\text{self}}, \quad (7)$$

with

$$V_{ij}^{\text{rs}} = (1 - \delta_{ij}) q_i q_j \frac{\text{erfc}(\kappa r_{ij})}{r_{ij}} \quad (8)$$

and

$$V_{ij}^{\text{ks}} = q_i q_j \left[\frac{1}{\pi L^3} \sum_{\mathbf{k} \neq 0} \frac{4\pi^2}{k^2} e^{-k^2/4\kappa^2} \cos(\mathbf{k} \cdot \mathbf{r}_{ij}) \right] \quad (9)$$

and

$$V_{ij}^{\text{self}} = -\delta_{ij} \frac{2\kappa}{\sqrt{\pi}}. \quad (10)$$

The real-space interactions could be further subdivided into distance classes.^{1,5} The above approach, introduced by Tuckerman and Berne,⁸ seems quite reasonable, considering the disparity in the distances over the terms summed in the real- and reciprocal-space parts. Recently, a formulation very similar to this one has been used by Procacci *et al.* in large-scale Ewald simulations of proteins.⁹

This particular split is implemented within the MTS-MC framework by subdividing the total potential energy of a molecule i into $V_S^{(i)}$ and $V_L^{(i)}$ in the following way:

$$V_i^{\text{pot}} = \sum_{j=0}^N (V_{ij}^{\text{LJ}} + V_{ij}^{\text{rs}} + V_{ij}^{\text{ks}} + V_{ij}^{\text{self}}), \quad (11)$$

where V_{ij}^{LJ} is the Lennard-Jones potential between oxygen atoms.^{7,17}

Many different potential break-ups can be implemented in the MTS-MC framework, as long as they obey detailed balance. An alternative break-up of the Ewald split introduced by Stuart, Zhou and Berne⁵ was also tested. The second split is very successful in MD simulations,¹ but did not perform as well within the MTS-MC framework; the split resulted only in a twofold speedup. Analysis of the failure of this split and ways of improving its performance are underway.

B. Scaling of Ewald parameters

For all system sizes, the initial $r_c \approx L/2$ (the cut-off radius for the real-space sum) and $k_c = 5$ (parameter defining summation range in the reciprocal space). As the system size increased, the speedup ratios for the MTS-MC method decreased for these choices of parameters because as we increase the size of the system, we make the real-space sum [the short range potential $\approx O(N^2)$] more computationally expensive. The computational time of the reciprocal-space sum only grows as $O(N)$. For an optimized Ewald sum, the order of the method scales at best as $O(N^{3/2})$. One way to maintain the speedup ratios for the MTS-MC algorithm is to scale both r_c and k_c such that the evaluation of the short-range potential becomes cheaper.

The optimal Ewald sum parameters are system dependent and are influenced by the trade-offs between accuracy and speed which depends on the computational implementation. For a comprehensive review of work on optimization of the Ewald sum refer to a survey of the Ewald summation techniques by Toukmaji and Board.¹⁶

In this section, we will use the approach introduced by Kolafa and Perram.²⁰ Kolafa and Perram derived formulas to estimate the standard deviations for the real-space and reciprocal-space (k -space) cut-off errors of the energy. The estimates for the Ewald errors for both real- and k -space energies are given by²⁰

$$\delta V^{\text{rs}} \approx \frac{Q}{L} \sqrt{\frac{r_c/L}{2}} \frac{\exp(-\kappa^2 r_c^2)}{\kappa^2 r_c^2}, \quad (12)$$

$$\delta V^{\text{ks}} \approx \frac{Q}{L} \frac{\sqrt{k_c}}{\kappa L} \frac{\exp(-\pi^2 k_c^2 / (\kappa L)^2)}{\pi^2 k_c^2 / (\kappa L)^2}, \quad (13)$$

where $Q = \sum_i q_i^2$, L is the box length, κ is the screening parameter, and r_c and k_c are the cutoffs in the real- and reciprocal-space. The above formulation suggests that the best choice of κ is when these errors are the same:

$$\kappa = \sqrt{\frac{\pi k_c}{r_c L}}. \quad (14)$$

Then, if Eq. (14) is substituted into the formulas for the errors in the energies,^{20,21}

$$\delta V^{\text{rs}} \approx \delta V^{\text{ks}} \approx \frac{\exp(-\pi k_c r_c / L)}{\pi k_c r_c / L}. \quad (15)$$

Thus, when r_c is multiplied and k_c is divided by the same scaling factor $R_s \in [0,1]$, the same error is achieved because the product $(r_c \cdot k_c)$ does not change.

For larger systems like biomolecular complexes, it would be more efficient to use methods that utilize FFT (fast Fourier transforms) to calculate the reciprocal part of the Ewald sum, making the calculation of real-space sum of order $O(N)$. Implementation of these techniques could improve the computational efficiency in absolute terms for both MC methods, while retaining computational speedups of MTS-MC to a lesser degree. The exact speedups would have to be investigated with computational experiments.

IV. RESULTS

A. Simulation details

To demonstrate that the real-/reciprocal-space split of MTS-MC is more efficient than MMC, we applied both algorithms to liquid water consisting of $N=108$, 256, and 500 molecules interacting through the SPC water model at 300 K and a density of 1.0 g/ml. The box lengths are $L_{108}=14.785$ Å, $L_{256}=19.713$ Å, and $L_{500}=24.641$ Å. The Ewald parameters for a system of $N=108$ molecules was taken as $r_c=L_{108}/2=7.393$ Å and $k_c=5$. The Ewald sum screening parameter, κ , was calculated using Eq. (14). All Lennard-Jones and real-space Coulomb interactions are terminated beyond $r_c=L_{108}/2$ for all the system sizes in both algorithms. Then, in order to preserve precision and accuracy of the Ewald summation, we have to divide the k_c values by a different scaling factor R_s for each system size (as described in Sec. III B): For $N=108$, $R_s=1.00$; for $N=256$, $R_s=L_{108}/L_{256}=0.75$; for $N=500$, $R_s=L_{108}/L_{500}=0.60$.

Ten simulations were started from different equilibrated water configurations for all values of N . The MMC runs were compared with the MTS-MC ($n=10$) runs (n is the MTS-MC splitting parameter). The simulations for 108 water molecules were 500 000 passes long; the data was collected every two passes; and configurations were saved every 20 passes. The simulations for 256 water molecules were 250 000 passes long; the data was collected every two passes; and configurations were saved every 20 passes. The simulations for 500 water molecules were 100 000 passes long; the data was collected every two passes; and configurations were saved every 20 passes.

The CPU time for one MC step in MMC and one “L-move” in MTS-MC are not equivalent. We define “the raw CPU speedup” as the ratio of CPU times by dividing the actual CPU time for a pass by CPU(MMC), obtaining τ . Thus, “the raw CPU speedup” for the MMC method is $\tau=\text{CPU}(\text{MMC})/\text{CPU}(\text{MMC})=1$ per MC pass, and for the MTS-MC method is $\tau=\text{CPU}(\text{MTS-MC})/\text{CPU}(\text{MMC})$ per MC pass. All the correlations are expressed as functions of τ relating the speedup ratios between the methods in the actual time that it takes to perform the calculations.

In all simulations, we adopt the point of view of Rao *et al.*^{22,23} that the optimum step size is the one that maximizes the translational and rotational diffusion. We optimized the step size for both methods, and used the optimum acceptance rates for each algorithm through the paper. The translational moves are accomplished by simple displacement and the rotational moves are performed using the quaternion procedure previously used in Monte Carlo by Vesely²⁴ and Trosset *et al.*²⁵

For water simulations, the optimized acceptance ratio was 30% for all system sizes (Strauch and Cummings²⁶ used 40% acceptance ratio for MMC calculations of a system of equal size). The acceptance ratio for the short-range potential in the MTS-MC simulation is about equivalent to the acceptance ratio in the MMC simulations; the long-range potential acceptance ratio is very high about 90%.

TABLE I. Average of the potential energy in kcal/mol per water molecule for three system sizes from MMC and MTS-MC ($n=10$) simulations.

No. of waters	Method	Energy	Exp. energy
108	MMC	-9.8811 ± 0.0037	-9.92^a
	MTS-MC	-9.8792 ± 0.0036	
256	MMC	-9.8809 ± 0.0032	
	MTS-MC	-9.8775 ± 0.0016	
500	MMC	-9.8755 ± 0.0043	
	MTS-MC	-9.8781 ± 0.0031	

^aReference 29.

B. Discussion

In Table I we present the average potential energies along with the experimental data for three system sizes. From the results presented, the MTS-MC simulations show good agreement with the results from MMC runs, both methods yielding accurate predictions for the energies, confirming that the new algorithm does not affect the accuracy of the methodology.

The radial distribution functions $g^{\text{OO}}(r)$, $g^{\text{OH}}(r)$, $g^{\text{HH}}(r)$ are shown in Fig. 1. All the curves are indistinguishable for both methods. The dipole–dipole orientational correlation function was calculated according to²⁷

$$c(r) = \frac{1}{\rho^2 g(r)} \left\langle \sum_{\alpha} \sum_{\beta \neq \alpha} \mathbf{e}_{\alpha} \cdot \mathbf{e}_{\beta} \delta(r - r_{\alpha\beta}) \right\rangle, \quad (16)$$

$$c(r) = 0 \quad \text{at} \quad g(r) = 0, \quad (17)$$

where $\mathbf{e}_{\beta}(\tau) = \boldsymbol{\mu}^{\beta} / |\boldsymbol{\mu}^{\beta}|$ is the unit vector pointing in the direction of the dipole moment of molecule β at τ , $g(r)$ is the radial distribution functions $g^{\text{OO}}(r)$, ρ is the number density, and $r_{\alpha\beta}$ the minimum image between molecules α and β . The dipole–dipole orientational correlation functions are displayed in Fig. 2. Again, the comparison is good, especially with regard to the peak values and positions. For both methods, the first neighbors of a water molecule exhibit a much stronger alignment with that of the central molecule than

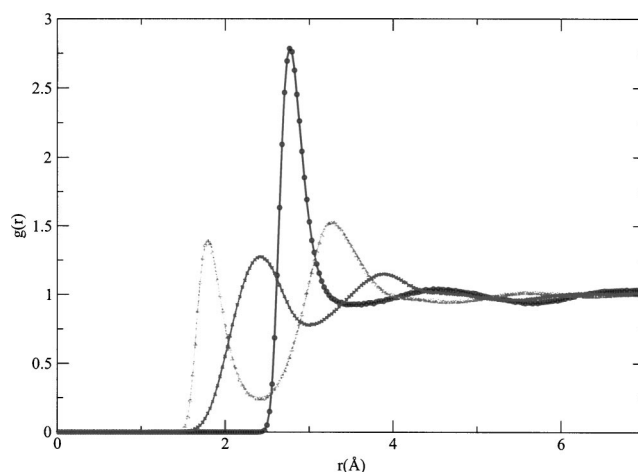


FIG. 1. The radial distribution function $g_{\text{OO}}(r)$, $g_{\text{OH}}(r)$, and $g_{\text{HH}}(r)$ at 300 K and $\rho=1.0$ g/cc from the MMC (solid lines) and MTS-MC (symbols) runs of 500 water molecules.

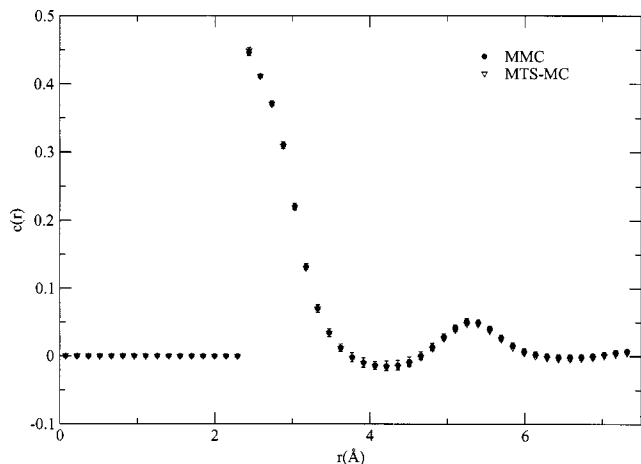


FIG. 2. The dipole-dipole orientational distribution function $c(r)$ averaged over several MMC (filled circles) and MTS-MC (empty triangles) runs of 500 water molecules with error bars.

with the second shell molecules, resulting in a first correlation peak at 2.4–2.5 Å (height at 0.45). A second correlation peak occurs at 5.3–5.4 Å (height at 0.06) for both cases and both methods. The correlation is positive almost everywhere and converges smoothly to zero. These results agree well with the results obtained by Hunenberger and van Gunsteren from molecular-dynamics simulations of SPC water.²⁸ And also they are in qualitative agreement with the MMC results for SPC water reported by Strauch and Cummings.²⁶

The translational diffusion coefficient for each method is obtained from the mean-square displacement^{22,23}

$$\langle \Delta r^2(\tau) \rangle = \frac{1}{T - \tau_{\text{MAX}}} \sum_{t=1}^{T - \tau_{\text{MAX}}} \frac{1}{N} \sum_{i=1}^N [\mathbf{r}_i^{\text{COM}}(t + \tau) - \mathbf{r}_i^{\text{COM}}(t)]^2, \quad (18)$$

where $\mathbf{r}_i^{\text{COM}}(t) = (\sum_{\alpha=1}^{n_a} m_{\alpha} \mathbf{r}_{i\alpha}) / \sum_{\alpha=1}^{n_a} m_{\alpha}$ is the position vector of the center-of-mass (COM) of a molecule at t (n_a is the number of atoms in the molecule and m_{α} is the mass of an atom), τ_{MAX} is the maximum length of τ , i.e., the overall length of the correlation function, and N is the number of molecules (or particles).

In Table II we show the speedup for MTS-MC as a function of system size. We define diffusion adjusted speedup (DAS) as “the raw CPU speedup” (defined in Sec. IV A) multiplied by the ratio of the diffusion constants, $D_{\text{MTS}}/D_{\text{MMO}}$.² The speedups range from 4.5 to 7.5 for systems with 108–500 waters. For larger system, the ratio of the CPU time for real-space versus reciprocal space calculations decreases, making MTS-MC more efficient than standard MC. In Table III we compare DAS for different values of the splitting parameter n for $N=500$ waters. As for Lennard-

TABLE II. Diffusion adjusted speedup (DAS) for MTS-MC as a function of system size. All the MTS-MC simulations were performed with splitting parameter $n=10$.

No. of waters	108	256	500
DAS	4.5	4.6	7.5

TABLE III. Diffusion adjusted speedup (DAS) for MTS-MC as a function of splitting parameter n from simulations with $N=500$.

n	5	10	20	30	40
DAS	5.8	7.5	7.7	7.3	6.3

Jones system,² the saturation of the speedup (DAS) occurs for $n=20$. Thus, over $n=20$, the diffusion slows down with increasing n , at the same time, the scaling with system size improves.

The rotational diffusion was assessed by looking at the angle of rotation of the molecular dipole moment vector,⁷

$$\langle \cos \theta(\tau) \rangle = \frac{1}{N} \sum_{\alpha} \left\langle \frac{\boldsymbol{\mu}^{\alpha}(\tau) \cdot \boldsymbol{\mu}^{\alpha}(0)}{|\boldsymbol{\mu}^{\alpha}|^2} \right\rangle, \quad (19)$$

and the normalized autocorrelation function of the total dipole polarization,⁷

$$\Phi(\tau) = \frac{\langle \mathbf{M}(\tau) \cdot \mathbf{M}(0) \rangle}{\langle \mathbf{M}(0) \cdot \mathbf{M}(0) \rangle}, \quad (20)$$

where $\boldsymbol{\mu}^{\alpha}(\tau)$ is the dipole moment of a molecule and $\mathbf{M}(\tau) = \sum_{\alpha=1}^N \boldsymbol{\mu}^{\alpha}(\tau)$ is the total dipole moment of the system at τ . The molecular dipole moment autocorrelation functions are shown in Fig. 3 for $N=500$. Exponential fitting of the data from the MMC and MTS-MC ($n=5$) simulations shows that the MTS-MC ($n=10$) rotational autocorrelation functions converge faster than the MMC functions with speedup ratios of 8 for $N=500$. The rotational correlations decay only slightly faster for $n=10$ and 20 than for $n=5$. The total dipole moment autocorrelation functions are displayed in Fig. 4. The speedup ratios of the MTS-MC ($n=10$) over the MMC for the total dipole moment autocorrelation functions are same as for the molecular dipole moment autocorrelation function, eight times faster for $N=500$.

The autocorrelation functions of the potential energy fluctuations are shown in Fig. 5 for $N=500$. After scaling the data, the speedup ratios for the MTS-MC follow the same behavior as the momentum correlation functions reported above.

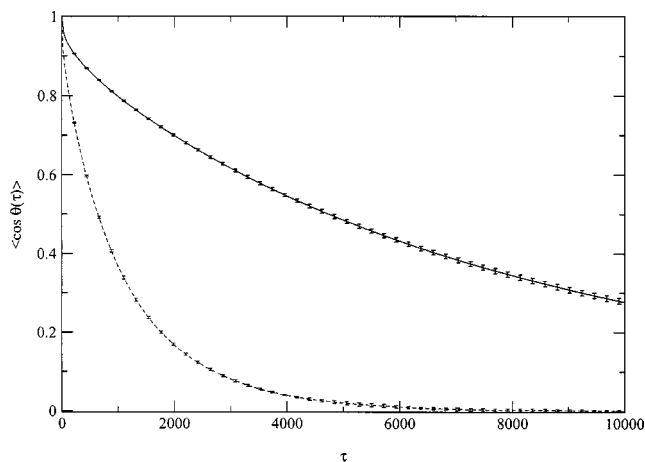


FIG. 3. Molecular dipole autocorrelation function from the MMC (solid line) and MTS-MC (dashed line) runs of 500 water molecules.

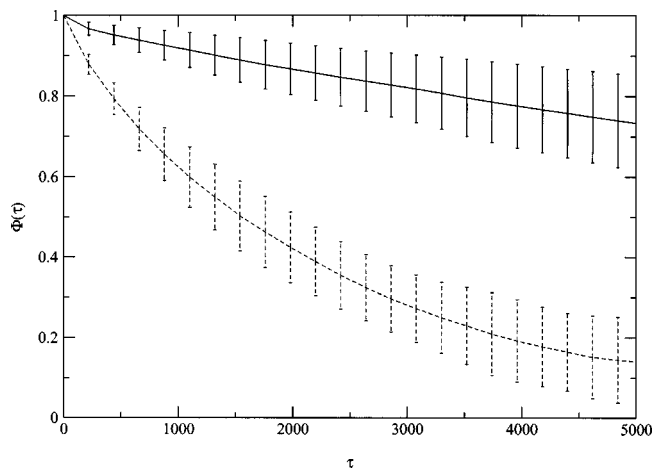


FIG. 4. Total dipole autocorrelation function from the MMC (solid line) and MTS-MC (dashed line) simulations of 500 water molecules.

The values for dielectric constant calculated are 35.25 ± 7.88 for MMC and 74.51 ± 11.24 for MTS-MC ($n=10$) after 50 000 passes for $N=500$. The experimental value of dielectric constant for water is 78.54 at 298.15 K and 76.60 at 303.15 K.²⁹ Previously reported dielectric constant values from computational simulations of SPC water at 300 K are 68.9 ± 4.2 (MD for 128 SPC waters), 73.3 ± 5.3 (MD for 250 SPC waters),²⁸ and 61 ± 31 (MMC for 108 SPC waters).²⁶ As evident from Fig. 6, the dielectric constant obtained using the MTS-MC ($n=10$) converges about eight times faster to the computational value (MD) and experimental value than in MMC simulations.

V. CONCLUSIONS

We have used a recently developed Monte Carlo algorithm, the multiple "time scale" Monte Carlo (MTS-MC),² to simulate the SPC water model with two different splits of the Ewald sum. In MTS-MC method, the potential is separated into two parts, one that varies quickly and one that

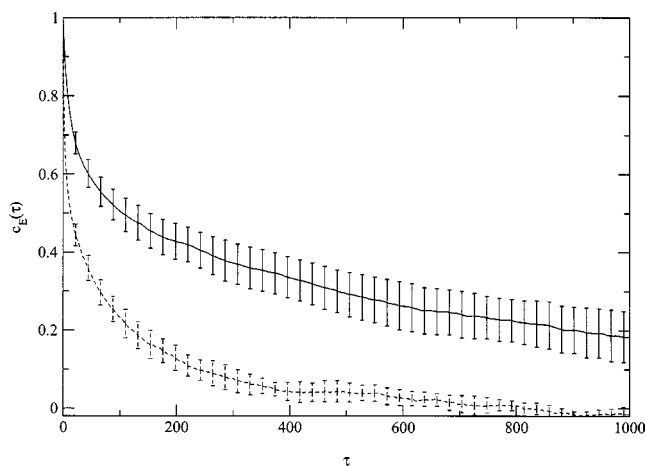


FIG. 5. Potential energy fluctuation autocorrelation function from the MMC (solid line) and MTS-MC (dashed line) runs of 500 water molecules.

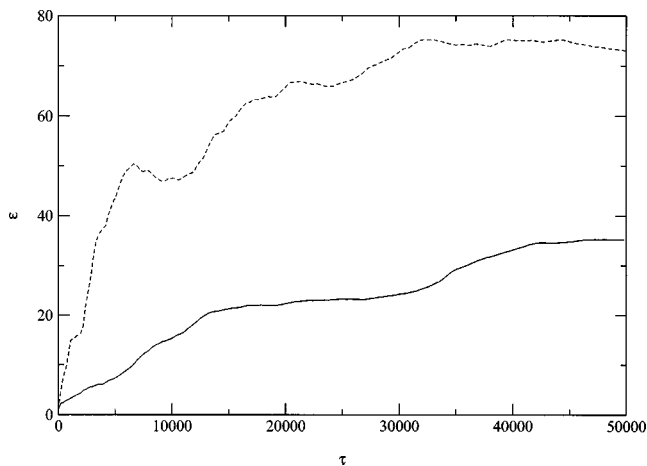


FIG. 6. The dielectric constant from the MMC (solid line) and MTS-MC (dashed line) simulations of 500 water molecules.

varies slowly as a function of the coordinates. The algorithm is similar in spirit to the reversible RESPA algorithm,⁸ in which the savings in CPU time results from the fact that the slowly varying part of the Hamiltonian is evaluated less frequently than the quickly varying part. In our proposed MTS-MC method, n moves are made using an acceptance ratio constructed from the quickly varying part of the potential, and the resulting configuration is accepted or rejected using the slowly varying part. For the long-range acceptance ratio the old configuration is the one from before the n moves, which is the configuration that is kept in case of rejection. In the previous paper,² we have shown that such a procedure obeys detailed balance.

We have applied both MC schemes to simulations using the SPC water model with the Ewald sum. The energetic, transport, structural and dielectric properties were calculated and compared for both methods. Structural properties such as the radial distribution functions and the dipole-dipole orientation correlation functions proved to be identical for both methods (within statistical error). The good agreement between distance dependent properties calculated by the two methodologies suggests that MTS-MC is the method of choice when one wants to investigate this group of properties.

Compared to the classical MMC approach, the MTS-MC method accelerates relaxation properties by 4.5–7.5 for the MTS-MC ($n=10$) for systems with 108–500 water molecules. We define the speedup factor as the ratio between the computing time required to evaluate a particular property by the MMC method and the MTS-MC method.

The thermodynamic properties for the two methods are in complete agreement to within the statistical errors for the two systems considered. They agree well with the experimental values. The distributions of potential energies resemble each other and fit the Boltzmann distribution. The MTS-MC method accelerates the decorrelation of the autocorrelation function of potential fluctuations by up to eight times, depending on the size of the system.

The dielectric constant calculated from the MTS-MC

trajectories, converges faster than that calculated from MMC simulations.

We have shown that in order to achieve the same speedup for larger water system as for the original 108 waters, the real- and reciprocal-space cutoffs (r_c and k_c) had to be, respectively, decreased and increased. Decreasing cut off radius r_c and increasing the screening parameter κ puts more work into the reciprocal-space making the new method even faster.

Given that other Ewald implementations (PME, P3ME, etc.)^{1,11-16} evaluate the reciprocal-space contribution more efficiently than the standard Ewald, it is likely that the speedup offered by MTS-MC relative to standard MC would decrease. Nevertheless, we think that the speedup would be considerable using standard MTS-MC. Furthermore, since MTS-MC offers additional flexibility in the break-up used, such as the fact that energy conservation is not a restriction (as in RESPA);³⁻⁶ moreover with the possibility of multi-level breakups, we are confident that a version of MTS-MC can be constructed to improve the efficiency of other applications of Ewald summation.

ACKNOWLEDGMENTS

We thank Harry A. Stern and Claudio J. Margulis for many useful discussions. This work was supported by Grant No. CHE-00-76279 from the National Science Foundation.

¹R. Zhou, E. Harder, H. Xu, and B. J. Berne, *J. Chem. Phys.* **115**, 2348 (2001).

²B. Hetényi, K. Bernacki, and B. J. Berne, *J. Chem. Phys.* **117**, 8203 (2002).

³M. Tuckerman, B. J. Berne, and G. J. Martyna, *J. Chem. Phys.* **97**, 1990 (1992).

⁴J. C. Sexton and D. H. Weingarten, *Nucl. Phys. B* **380**, 665 (1992).

⁵S. J. Stuart, R. Zhou, and B. J. Berne, *J. Chem. Phys.* **105**, 1426 (1995).

⁶R. Zhou and B. J. Berne, *J. Chem. Phys.* **103**, 9444 (1995).

⁷M. P. Allen and D. J. Tildesley, *Computer Simulation of Liquids* (Clarendon Press, Oxford, 1987).

⁸M. Tuckerman and B. J. Berne, *J. Chem. Phys.* **95**, 8362 (1991).

⁹P. Procacci and M. Marchi, *J. Chem. Phys.* **104**, 3003 (1996).

¹⁰P. Procacci, T. Darden, and M. Marchi, *J. Phys. Chem.* **100**, 10464 (1996).

¹¹T. Darden, D. York, and L. Pederson, *J. Chem. Phys.* **98**, 10089 (1993).

¹²U. Essmann, L. Perera, M. Berkowitz, T. Darden, H. Lee, and L. Pederson, *J. Chem. Phys.* **103**, 8577 (1995).

¹³R. Hockney and J. Eastwood, *Computer Simulations using Particles* (McGraw-Hill, New York, 1981).

¹⁴J. Eastwood, R. Hockney, and D. Lawrence, *Comput. Phys. Commun.* **19**, 215 (1980).

¹⁵B. Luty, M. Davis, I. Tironi, and W. van Gunsteren, *Mol. Simul.* **14**, 11 (1994).

¹⁶A. Y. Toukmaji and J. J. A. Board, *Comput. Phys. Commun.* **95**, 73 (1995).

¹⁷H. J. C. Berendsen, J. P. M. Postma, W. F. van Gunsteren, and J. Hermans, in *Intermolecular Forces: Proceedings of the Fourteenth Jerusalem Symposium on Quantum Chemistry and Biochemistry*, edited by B. Pullman (Reidel, Dordrecht, 1981), p. 331.

¹⁸P. Ewald, *Ann. Phys. (Leipzig)* **64**, 253 (1921).

¹⁹D. Frenkel and B. Smit, *Understanding Molecular Simulation: From Algorithms to Applications* (Academic, New York, 1996).

²⁰J. Kolafa and J. W. Perram, *Mol. Simul.* **9**, 351 (1992).

²¹H. A. Stern, *Polarizable Potential Energy Functions for Molecular Simulation*, Ph.D. thesis, Columbia University, New York (2001).

²²M. Rao, C. Pangali, and B. J. Berne, *Mol. Phys.* **37**, 4056 (1979).

²³M. Rao, C. Pangali, and B. J. Berne, *Mol. Phys.* **40**, 661 (1980).

²⁴F. J. Vesely, *J. Comput. Phys.* **47**, 291 (1982).

²⁵J. Y. Trosset and H. A. Scheraga, *Proc. Natl. Acad. Sci. U.S.A.* **20**, 412 (1999).

²⁶H. J. Strauch and P. T. Cummings, *Mol. Simul.* **2**, 89 (1989).

²⁷J. A. Barker and R. O. Watts, *Mol. Phys.* **26**, 789 (1973).

²⁸P. H. Hunenberger and W. F. Van Gunsteren, *J. Chem. Phys.* **108**, 6117 (1998).

²⁹W. J. Jorgensen, J. Chandrasekhar, J. D. Madura, R. W. Impey, and M. L. Klein, *J. Chem. Phys.* **79**, 926 (1983).